

Size dependence of discrete change in magnetization in single crystal of chiral magnet $\text{Cr}_{1/3}\text{NbS}_2$

Cite as: J. Appl. Phys. **120**, 143901 (2016); <https://doi.org/10.1063/1.4964427>

Submitted: 01 July 2016 . Accepted: 25 September 2016 . Published Online: 11 October 2016

K. Tsuruta, M. Mito, Y. Kousaka, J. Akimitsu, J. Kishine, Y. Togawa, and K. Inoue



View Online



Export Citation



CrossMark

ARTICLES YOU MAY BE INTERESTED IN

[Spin structure of the anisotropic helimagnet \$\text{Cr}_{1/3}\text{NbS}_2\$ in a magnetic field](#)

Applied Physics Letters **105**, 072405 (2014); <https://doi.org/10.1063/1.4893567>

[Role of structural factors in formation of chiral magnetic soliton lattice in \$\text{Cr}_{1/3}\text{NbS}_2\$](#)

Journal of Applied Physics **116**, 133901 (2014); <https://doi.org/10.1063/1.4896950>

[Investigation of structural changes in chiral magnet \$\text{Cr}_{1/3}\text{NbS}_2\$ under application of pressure](#)

Journal of Applied Physics **117**, 183904 (2015); <https://doi.org/10.1063/1.4919833>

Applied Physics Reviews
Now accepting original research

2017 Journal
Impact Factor:
12.894

Size dependence of discrete change in magnetization in single crystal of chiral magnet $\text{Cr}_{1/3}\text{NbS}_2$

K. Tsuruta,^{1,a),b)} M. Mito,^{1,2} Y. Kousaka,^{2,3} J. Akimitsu,^{2,3} J. Kishine,^{2,4} Y. Togawa,^{2,5} and K. Inoue^{2,3,6}

¹Graduate School of Engineering, Kyushu Institute of Technology, Kitakyushu 804-8550, Japan

²Center for Chiral Science, Hiroshima University, Higashihiroshima 739-8526, Japan

³Graduate School of Science, Hiroshima University, Higashihiroshima 739-8526, Japan

⁴Graduate School of Arts and Sciences, The Open University of Japan, Chiba 261-8586, Japan

⁵Graduate School of Engineering, Osaka Prefecture University, Sakai 599-8570, Japan

⁶Institute for Advanced Materials Research, Hiroshima University, Higashihiroshima 739-8526, Japan

(Received 1 July 2016; accepted 25 September 2016; published online 11 October 2016)

The single crystal of a chiral magnet $\text{Cr}_{1/3}\text{NbS}_2$ exhibits discrete changes in magnetization (M) in response to changes in magnetic field (H) triggered by the formation of a chiral soliton lattice (CSL). In order to provide evidence of this phenomenon, the study of the size effect is indispensable. We investigated the effects of size on this phenomenon by the use of two single crystals, (A) and (B), whose crystal sizes along the c -axis were $110\ \mu\text{m}$ and $60\ \mu\text{m}$, respectively. First, in (A), the large jumps of M observed in the process of decreasing H exhibited inconsistent features, whereas the largest and second-largest jumps in (B) exhibited reproducibility for both the value of H and the magnitude of the M jumps. This confirms that these large jumps do not originate from the Barkhausen effect, as this effect would result in M jumps appearing at random values of H . When the system size of a sample becomes smaller, the features of the Barkhausen effect are suppressed. Second, as for the successive jumps observed in the H region where the rapid change in M is entirely seen for both the samples, the number of observed M jumps for (B) is more than that for (A). Indeed, the number of the domain wall due to the 2π -soliton in the CSL increases, as the c -axis length of the single crystal increases. However, a series of M jumps must appear in a limited H region below the critical field of the order of 2 kOe. The greater the number of M jumps, the more difficult the detection of the M jump will be in the H resolution of the present setup. Thus, the effects of size on the M jumps observed in the present setup can be understood within the framework of the CSL formation. *Published by AIP Publishing.* [<http://dx.doi.org/10.1063/1.4964427>]

I. INTRODUCTION

In chiral materials that break spatial inversion symmetry, the magnetic properties are characterized by a competition between symmetric Heisenberg and antisymmetric Dzyaloshinskii-Moriya (D-M) exchange interactions, resulting in a chiral helimagnetic structure, as shown in Fig. 1(a).^{1,2} When a dc magnetic field (H) is applied perpendicular to the chiral helical axis of the helimagnetic structure, uniform space-modulation of the spin phase is broken, resulting in the stabilization of a type of superlattice structure called the chiral soliton lattice (CSL), as shown in Fig. 1(b).³⁻⁵ The pitch of the CSL and the number of the 2π spin rotations are controlled by H , finally leading to the forced-ferromagnetic (FFM) state, as shown in Fig. 1(c).^{5,6} Theoretical study of the finite system indicates that the change in the CSL state accompanies a discrete change in magnetization (ΔM) as well as a continuous change in magnetization.⁷ Recently, for a micro-sized sample of a chiral magnet, $\text{Cr}_{1/3}\text{NbS}_2$, in which magnetic solitons are confined, it was reported that the electrical resistance changed discretely against a change in H , with the discretized change of soliton number being directly observed by the Lorentz

microscopy.⁸ Additionally, we reported that M became discrete for a change in H in a single crystal of $\text{Cr}_{1/3}\text{NbS}_2$ with sub-millimeter thickness along c -axis ($0.12\ \text{mm}$), within which magnetic solitons were reliably confined by the grain boundaries.⁹ There are two types of ΔM s: large ΔM s are observed in the process of decreasing H from the FFM state, and successive ΔM s appear in the H region where M changes rapidly with respect to H . The former occurred inconsistently; both the value of H for ΔM and the value of ΔM itself were not reproducible, which is qualitatively similar to that predicted by the Barkhausen effect. Subsequently, we define that ΔM s of the Barkhausen type depend on the measurement, suggesting that both the magnitude of the ΔM and its magnetic field depend on the measurements. On the other hand, successive ΔM s of the CSL are intrinsically independent of the measurements and are reproducible in both the magnitude of ΔM and its magnetic field. In this paper, to experimentally prove that both types of ΔM are related to the CSL formation, we investigate the effects of crystal size on both types of ΔM s via magnetization measurement of two single crystals.

II. EXPERIMENTS

$\text{Cr}_{1/3}\text{NbS}_2$ has a layered hexagonal structure of the 2H-type NbS_2 intercalated with Cr atoms and belongs to the

^{a)}Electronic mail: tsuruta@spring8.or.jp

^{b)}Current address: Japan Synchrotron Radiation Research Institute (JASRI), Sayo, Hyogo 679-5148, Japan.

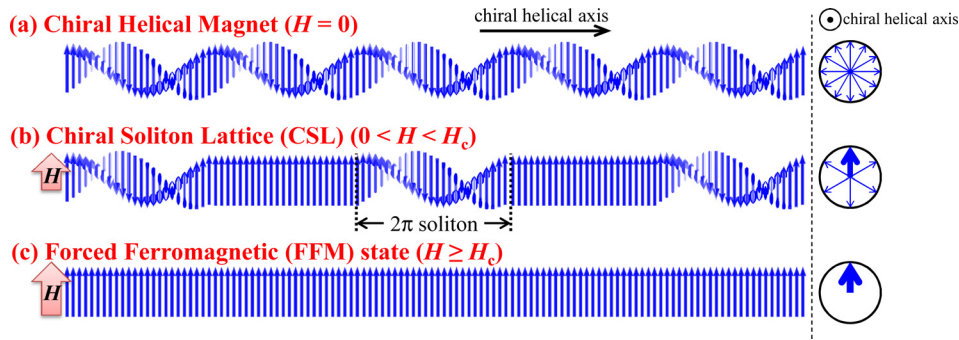


FIG. 1. Spin structure of the chiral magnet in the magnetic field H , applied perpendicular to the chiral helical axis; (a) chiral helical magnet at zero magnetic field, (b) chiral soliton lattice (CSL) in the finite H and (c) forced ferromagnetic (FFM) state in H greater than a critical field H_c . Spin structures viewed along the direction parallel to the chiral helical axis are displayed in the right side of Fig. 1. The line weight of the arrows qualitatively reflects the magnitude of the total magnetic moment along a direction.

space group $P6_322$. The chiral helical axis of the structure is the c -axis, and the lattice parameters at room temperature are $a = 5.75 \text{ \AA}$ and $c = 12.12 \text{ \AA}$.¹⁰ The periodic length of the helimagnetic structure, when no magnetic field is applied, is 48 nm .^{5,10} The single crystal was grown by a chemical transport technique.¹¹ For this experiment, we prepared two single crystals of $\text{Cr}_{1/3}\text{NbS}_2$ and the volumes of which (the surface area of the ab plane, S_{ab} , \times the length of the single crystal along the c -axis, L_c) are $0.26 \text{ mm}^2 \times 0.11 \text{ mm}$ for sample (A) and $0.16 \text{ mm}^2 \times 0.06 \text{ mm}$ for sample (B). According to calculations, the single crystals should contain approximately 2300 and 1300 2π -solitons at zero H , respectively. The magnetic ordering temperature of the present crystals was estimated to be 130 K by the AC magnetic susceptibility measurements.

The magnetization of $\text{Cr}_{1/3}\text{NbS}_2$, M , was measured as a function of H at temperature, T , of 5 K using a superconducting quantum interference device (SQUID) magnetometer. Field H was applied perpendicularly to the helical c -axis. H was increased and decreased by 0.15 Oe, which is the smallest increment permitted by the apparatus. The diamagnetic contribution of the sample holder, which was mainly made of epoxy resin, was subtracted from the measured M .

III. EXPERIMENTAL RESULTS AND DISCUSSION

Figure 2 shows all the M/M_s - H curves produced using the samples (A) and (B) at $T = 5 \text{ K}$ (squares and circles, respectively). The data produced by the process of increasing and decreasing H are indicated by closed and opened symbols, respectively. The overall observed behavior is consistent with that reported in the literature.^{6,9,10,12} M exhibits a remarkable increase just before it becomes saturated, and its H region has a definite hysteresis.¹⁰ The longitudinal axis is normalized by the saturated magnetization (M_s). We define a critical field H_c , at which M becomes saturated and simultaneously the hysteresis disappears as H increases; H_c was estimated to be approximately 2.4 kOe at $T = 5 \text{ K}$ for both (A) and (B). The magnetic ordering temperature and the above critical field H_c are indexes for evaluating the crystal's quality, and hence, based on a series of consistent results, we consider that (A) and (B) are of the same level of crystal

quality. Indeed, the two samples exhibit consistent M/M_s - H curves over the entire magnetic field range.

Figures 3 and 4 show the enlarged M/M_s - H curves for decreasing H at $T = 5 \text{ K}$ in (A) and (B), respectively. The M/M_s regions in Figs. 3 and 4 correspond to an H/H_c value in the range $0.79 \leq H/H_c \leq 0.92$. The insets in Fig. 3 show further enlarged M/M_s - H curves in the region of $0.965 \leq M/M_s \leq 0.990$. In Figs. 3 and 4, several prominent M jumps are observed. In (A), a series of jumps appears at seemingly random values of H , whereas the largest and the second largest jumps in (B) occur reliably at the same values of H and consistently increase by the same magnitude of M . The largest jump appears at $H = 1.924 \pm 0.001 \text{ kOe}$, with the second-largest at $H = 1.903 \pm 0.001 \text{ kOe}$. For H values from 1.9 to 2.2 kOe, the number of jumps in M for (A) is more than twice that for (B): the magnitude of the largest jump in (B) is approximately 4% of M_s (corresponding to approximately fifty 2π -solitons in M within the CSL formation). In (A), the corresponding value is at most 1% of M_s . This large jump has also been recognized at a fixed value of H in the magnetoresistance of micro-sized samples⁸ and is most probably an intrinsic phenomenon in systems where the CSL is spatially confined by certain factors, such as surface anisotropy,

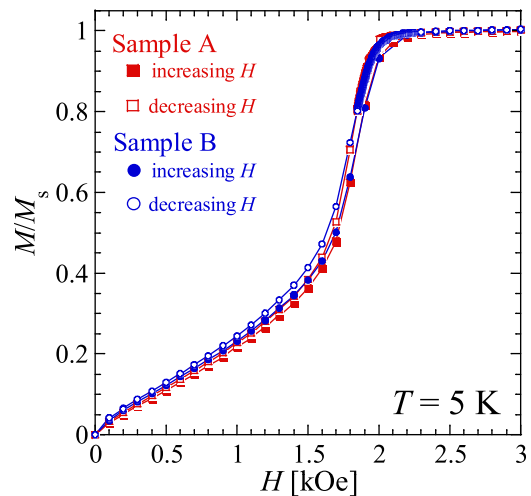


FIG. 2. Entire M/M_s - H curves of single crystal of $\text{Cr}_{1/3}\text{NbS}_2$ whose crystal sizes along c -axis are $110 \mu\text{m}$ (A) and $60 \mu\text{m}$ (B), respectively, at $T = 5 \text{ K}$. The longitudinal axis is normalized by the M_s .

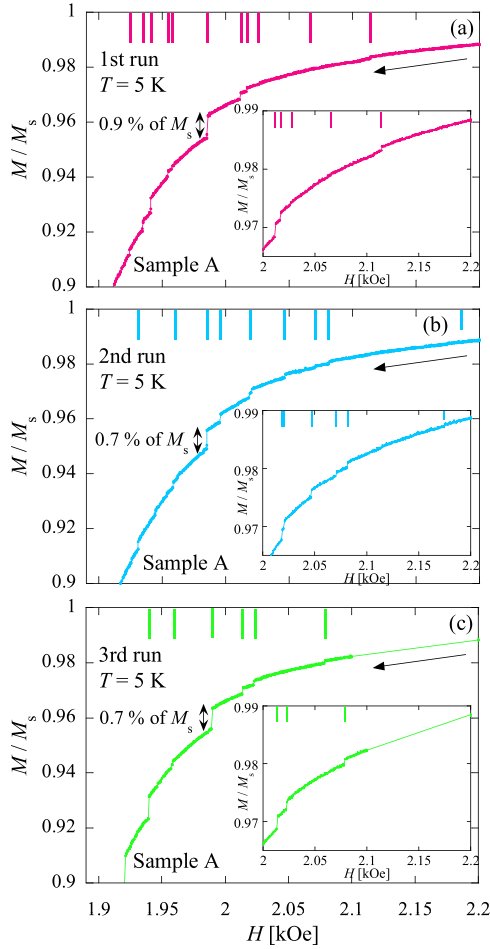


FIG. 3. Enlarged M/M_s - H curves of (A) in the process of decreasing H for $0.79 \leq H/H_c \leq 0.92$ at $T = 5$ K. Inset figures show the enlarged M/M_s - H curves in the region of $H = 2.0$ – 2.2 kOe. Figs. 3(a)–3(c) show the data of the 1st run, the 2nd run, and the 3rd run, respectively. The direction of the change in H is indicated by the arrows. Lines in the top side of each graph indicate the value of H , in which distinct M jumps appear. In particular, for significant M jumps, the ratio of the magnitude of the jump against M_s is shown.

domain walls and pinning due to structural defects, etc. It indicates that inserting the 2π -solitons into the FFM state requires overcoming a remarkable energy barrier and that this trend is emphasized in the smaller system.

Figure 5 shows the enlarged M/M_s - H curves for (B) in the region of $0.975 \leq M/M_s \leq 0.990$. A small jump can be seen at approximately $H = 1.976 \pm 0.06$ kOe, prior to the appearance of the largest jump observed, while decreasing H , for all runs. Its H value depends on the run, and the deviation of 0.06 kOe is sixty times as large as that in the largest jump. The magnitude of the small jump is approximately 0.2% of M_s , corresponding to a few 2π -soliton in the case where there is no continuous change in M . When focusing on the largest and second-largest M jumps, the features of the Barkhausen effect are not seen. However, even in (B), the small jump prior to the largest jump exhibits the Barkhausen effect assisted by the CSL.

Figures 6 and 7 show the enlarged M/M_s - H curves for (A) and (B), respectively, in the process of decreasing H . These were taken for a range of $0.773 \leq H/H_c \leq 0.779$ and $0.783 \leq H/H_c \leq 0.790$, where the rapid change in M is

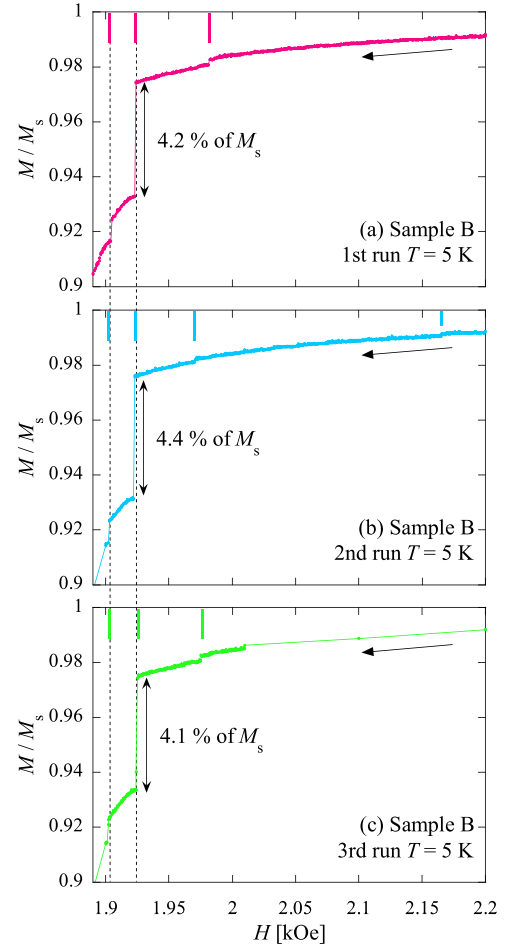


FIG. 4. Enlarged M/M_s - H curves of (B) in the process of decreasing H for $0.77 \leq H/H_c \leq 0.92$ at $T = 5$ K. Figs. 4(a)–4(c) show the data of the 1st run, the 2nd run, and the 3rd run, respectively. The direction of the change in H is indicated by the arrows. Lines in the top side of each graph indicate the value of H , in which distinct M jumps appear. In order to confirm reproducibility of a series of measurements, dotted lines show where the prominent jumps appear.

completely seen. The M/M_s - H curve consists of the linear contribution M_{lin} and the discrete change. The latter is more prominently observed in the process of decreasing H than in that of increasing H , which is consistent with our previous observation.⁹ Figures 6 and 7 present that the M_{lin} in (A) is larger than that in (B) and the number of jumps in (A) is approximately a half of that in (B). First, we discuss the size effect on the latter.

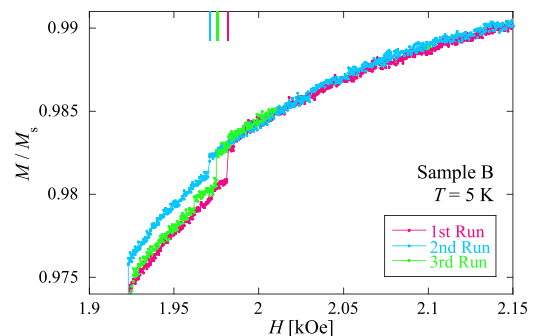


FIG. 5. Enlarged M/M_s - H curves for (B) in the process of decreasing H for $0.97 \leq M/M_s \leq 0.995$ at $T = 5$ K. Three guide-lines represent the magnetic field, in which one distinct M jump appears in each run.

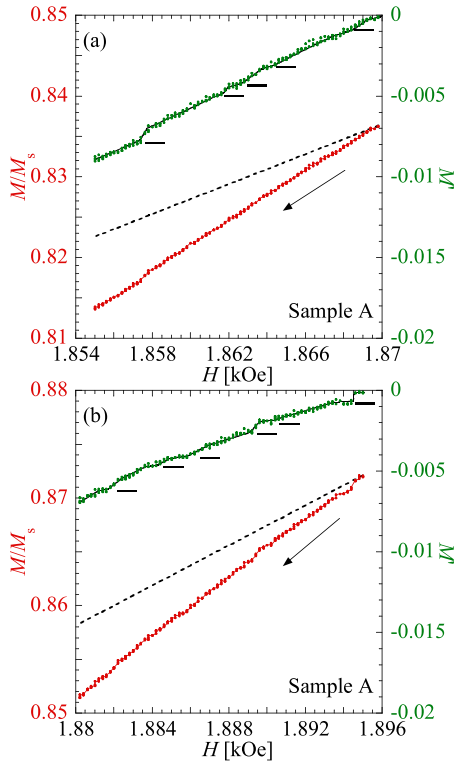


FIG. 6. Enlarged M/M_s - H curves for (A) in the process of decreasing H for $0.77 \leq H/H_c \leq 0.79$ at $T = 5$ K. The dotted lines present the linear contribution M_{lin} ($dM_{\text{lin}}/dH \sim \text{constant}$) and $M' = M/M_s - M_{\text{lin}}$. Deviation between the observed M/M_s and M_{lin} is presented as M' . The distinct M jumps are marked with the solid lines in the data of M' . The arrow indicates the direction of changing H .

Herein, let us consider how the number of 2π -soliton in the CSL theoretically changes as a function of the length of the single crystal along c -axis L_c . The number of 2π -soliton in the CSL decreases with decreasing L_c . However, in $\text{Cr}_{1/3}\text{NbS}_2$, a series of jumps must appear in a limited H region below $H_c \sim 2$ kOe. The larger the number of jumps, the greater the difficulty there will be in detecting the jumps within the same H region. The above experimental results demonstrate that the number of the discrete changes in M increases with decreasing L_c and the size effect observed here can be experimentally understood within the framework of the CSL formation. Second, we consider the size effect on M_{lin} . When the continuous change in M is considered in the narrow region, it could be approximated as a linear term against H . Consequently, the intrinsic M_{lin} in both (A) and (B) should be quantitatively the same. However M_{lin} in (A) is significantly larger than that in (B). Intrinsically, the number of the 2π -solitons for (A) should be about twice that in (B) because L_c for (A) is approximating twice that of (B). Indeed, many of the discrete change in M for (A) could not be distinguished from each other, so that M_{lin} in (A) is larger than that in (B). Finally, we discuss the experiment for smaller L_c . Over one-tenth of L_c for (A), a conventional SQUID magnetometer would not have sufficient accuracy to count the number of discrete changes in M . The measurement for smaller L_c requires another setup for the magnetic measurement. The single crystals used in this experiment should have certain anisotropy for chiral solitons such as surface anisotropy, domain walls, and pinning due to structural

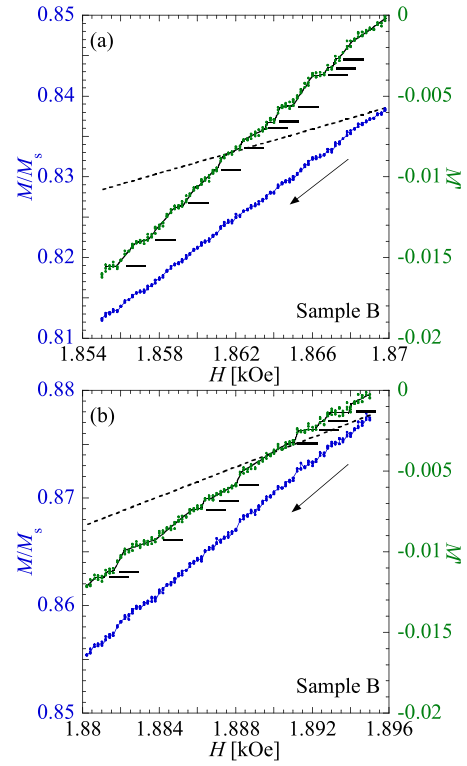


FIG. 7. Enlarged M/M_s - H curves for (B) in the process of decreasing H for $0.77 \leq H/H_c \leq 0.79$ at $T = 5$ K. The dotted lines present the linear contribution M_{lin} ($dM_{\text{lin}}/dH \sim \text{constant}$) and $M' = M/M_s - M_{\text{lin}}$. Deviation between the observed M/M_s and M_{lin} is presented as M' . The distinct M jumps are marked with the solid lines in the data of M' . The arrow indicates the direction of changing H .

defects, etc. It is an open problem to investigate the magnetization curve of the CSL in the case of small confinement of chiral solitons.

IV. CONCLUSION

We studied the effects of crystal size on the discrete change in magnetization of $\text{Cr}_{1/3}\text{NbS}_2$. As the crystal size along the c -axis decreases, the Barkhausen effect is suppressed in the large M jumps observed near the critical field. The number of successive M jumps observed in the H region, where the rapid change in M is entirely seen, increases with decreasing the crystal size along c -axis. The results presented support the hypothesis that a series of discrete changes in M observed in the single crystals, i.e., large jumps near the critical field as well as successive jumps in the field region far from the H_c , originates from the formation of the chiral soliton lattice.

ACKNOWLEDGMENTS

This work was supported by the Grants-in-Aid for Scientific Research, Grant Nos. (A) 22245023 and (S) 25220803, from the Ministry of Education, Culture, Sports, Science and Technology (MEXT), Japan. This work was also supported by the Center for Chiral Science in Hiroshima University (the MEXT program for promoting the enhancement of research universities, Japan) and the JSPS Core-to-Core Program, A. Advanced Research Networks.

- ¹I. E. Dzyaloshinskii, *J. Phys. Chem. Solids* **4**, 241 (1958).
- ²T. Moriya, *Phys. Rev.* **120**, 91 (1960).
- ³I. E. Dzyaloshinskii, *Sov. Phys. JETP* **20**, 665 (1965).
- ⁴J. Kishine, K. Inoue, and Y. Yoshida, *Prog. Theor. Phys. Suppl.* **159**, 82 (2005).
- ⁵Y. Togawa, T. Koyama, K. Takayanagi, S. Mori, Y. Kousaka, J. Akimitsu, S. Nishihara, K. Inoue, A. S. Ovchinnikov, and J. Kishine, *Phys. Rev. Lett.* **108**, 107202 (2012).
- ⁶Y. Togawa, Y. Kousaka, S. Nishihara, K. Inoue, J. Akimitsu, A. S. Ovchinnikov, and J. Kishine, *Phys. Rev. Lett.* **111**, 197204 (2013).
- ⁷J. Kishine, I. G. Bostrem, A. S. Ovchinnikov, and V. E. Sinitsyn, *Phys. Rev. B* **89**, 014419 (2014).
- ⁸Y. Togawa, T. Koyama, Y. Nishimori, Y. Matsumoto, S. McVitie, D. McGrouther, R. L. Stamps, Y. Kousaka, J. Akimitsu, S. Nishihara, K. Inoue, I. G. Bostrem, V. E. Sinitsyn, A. S. Ovchinnikov, and J. Kishine, *Phys. Rev. B* **92**, 220412 (2015).
- ⁹K. Tsuruta, M. Mito, Y. Kousaka, J. Akimitsu, J. Kishine, Y. Togawa, H. Ohsumi, and K. Inoue, *J. Phys. Soc. Jpn.* **85**, 013707 (2016).
- ¹⁰T. Miyadai, K. Kikuchi, H. Kondo, S. Sakka, M. Arai, and Y. Ishikawa, *J. Phys. Soc. Jpn.* **52**, 1394 (1983).
- ¹¹Y. Kousaka, Y. Nakao, J. Kishine, M. Akita, K. Inoue, and J. Akimitsu, *Nucl. Instrum. Methods Phys. Res., Sect. A* **600**, 250 (2009).
- ¹²N. J. Ghimire, M. A. McGuire, D. S. Parker, B. Sipoș, S. Tang, J.-Q. Yan, B. C. Sales, and D. Mandrus, *Phys. Rev. B* **87**, 104403 (2013).